Franziska Sophia Stolte*, Carmen Martínez Antón, Eric Invers Rubio, Eduard Guasch, Lluís Mont, Olaf Dössel, and Axel Loewe

Comparison of LGE-MRI and Local Impedance Data Recorded in Human Left Atria

https://doi.org/10.1515/cdbme-2024-2153

Abstract: Efficient personalized ablation strategies for treating atrial arrhythmias remain challenging. Discrepancies in identifying arrhythmogenic areas using characterization methods, such as late gadolinium enhanced magnetic resonance imaging (LGE-MRI) and electroanatomical mapping, require a comparative analysis of local impedance (LI) and LGE-MRI data. This study aims to analyze correlations as basis for improvement of treatment strategies. 16 patients undergoing left atrium (LA) ablation with LGE-MRI acquisition and LI data recording were recruited. LGE-MRI data and LI measurements were normalized to patient- and modality-specific blood pool references. A global mean shape was generated based on all patient geometries, and normalized local impedance (LI_N) and LGE-MRI image intensity ratio (IIR) data points were co-registered for comparison.

Data analysis comprised intra-patient and inter-patient assessments, evaluating differences in LI_N values among datasets categorized by their IIR. Due to substantial deviations in LI_N values, even within the same patient and IIR-category, discerning the presence or absence of a correlation was challenging, and no statistically significant correlation could be identified.

Our findings underscore the necessity for standardized protocols in data acquisition, processing, and comparison, to minimize unquantified confounding effects. While immediate substitution of LI for LGE-MRI seems improbable given the significant LI_N variations, this preliminary study lays the groundwork for systematic data acquisition. By ensuring data quality, a meaningful comparison between LI and LGE-MRI data can be facilitated, potentially shaping future strategies for atrial arrhythmia treatment.

Keywords: Cardiology, Electrophysiology, Atrial Tachycardia, Magnetic Resonance, Local Impedance

***Corresponding author: Franziska Sophia Stolte, Carmen Martínez Antón, Olaf Dössel, Axel Loewe,** Institute of Biomedical Engineering, Karlsruhe Institute of Technology (KIT), Kaiserstr. 12, 76131 Karlsruhe, Germany, e-mail: publications@ibt.kit.edu

Eric Invers Rubio, Eduard Guasch, Lluís Mont, Institut d'Investigacions Biomèdiques August Pi i Sunyer (IDIBAPS), Hospital Clínic, University of Barcelona, C/Roselló 149, 08036 Barcelona, Spain.

1 Introduction

Atrial arrhythmia affects 1 to 2% of the population, compromising cardiac function, and increasing the risk of thrombus formation [7]. Catheter ablation, a primary therapeutic approach, targets electrical isolation of pathogenic substrate. While pursuing individualized treatment strategies, their efficacy yields ambiguous outcomes [2]. Methods to characterize left atrium (LA) substrate exhibit discrepancies in identifying the location and extent of arrhythmogenic areas [6].

Late gadolinium enhanced magnetic resonance imaging (LGE-MRI) discerns substrates by highlighting scar tissue through substantially higher contrast agent concentration compared to healthy myocardium during the late enhancement phase [1]. Secondary effects of the contrast agent together with elevated time and cost requirements are the main drawback of this technique. Contrarily, local impedance (LI) measurements are employed to verify proper tissue contact by elevation over the blood pool value (LI_{BP}) and to assess successful lesion formation with a drop of 10 to 20% from its initial value [4]. As LI represents a reciprocal quantity to local conductivity, it holds the potential to characterize substrate based on its electrical properties, independent from a depolarization wave.

However, to our knowledge, a direct comparison between LI and LGE-MRI is lacking. Such a comparison holds promise in providing insights into the existence and extent of a potential correlation. Thus, this preliminary study seeks to elucidate relevant factors influencing the comparison of LI and LGE-MRI, identifying challenges to inform a study design incorporating adequate mitigation strategies.

2 Methods

2.1 Clinical Cohort - Data Collection

Clinical data were collected for 16 patients (6 female) with an average age of 66.53 $\pm$ 11.73 years diagnosed with atrial tachycardia (5 atrial flutter, 3 paroxysmal atrial fibrillation, 8 persistent atrial fibrillation) at Hospital Clínic, University of Barcelona. Patients underwent LA ablation procedures with either the IntellaNav Stablepoint™ or IntellaNav Mifi™ OI catheter, together with the Rhythmia HDx electroanatomical mapping system (Boston Scientific, Marlborough, MA, USA).

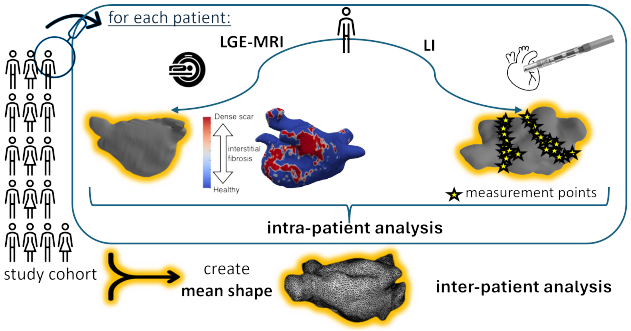

Fig. 1: Workflow for IIR and LI extraction and analysis. Geometries used for mean shape generation are marked yellow.

The pipeline of this preliminary study is shown in Figure 1. A pre-procedural LGE-MRI image was obtained from each patient no longer than two weeks prior to the ablation procedure, ensuring minimal structural changes in the heart between LGE-MRI acquisition and ablation.

LGE-MRI

The LGE-MRI data acquisition procedure is elaborated in detail by Caixal et al. [3]. The voxel size was 1.25 mm × 1.25 mm × 2.5 mm. IIR was derived by dividing the voxel values, post-processed using the ADAS 3D software (Galgo Medical S.L.), by their patient-specific blood pool value, representing the signal intensity of blood. Employing threshold values as defined by Benito et al. [1], the tissue was subsequently categorized into healthy (IIR $<$ 1.20), interstitial fibrosis (1.20 $\leq$ IIR $<$ 1.32), or dense scar (IIR $\geq$ 1.32).

LI Recordings

Data were collected based on the operator's discretion. The LA shell was recorded with a mapping catheter. During the consecutive ablation procedure, Direct Sense™ technology was employed to obtain measures of LI with a sampling frequency of 20 Hz, along with contact force if available. Remapping was performed as deemed necessary. LI values were acquired for ablation points, focusing on dynamic changes during ablation, rather than collecting a complete LI map of the LA.

2.2 LI Data Processing

In this paper, the term "ablation point" refers to the areas where ablation was performed, each containing several data points called samples. Each sample comprises the location of each electrode, a LI value, and is assigned to the latest recorded shell map based on its specific timestamp. While recordings included samples for the entire ablation, during data processing we extracted only normalized pre-ablative values representing the untreated substrate, available at ablation points.

Blood Pool Value (LI_{BP})

The LI_{BP} serves as a reference value, used for normalization. To calculate a single LI_{BP} value per patient, samples corresponding to each LA shell map with consecutive ablation points were accumulated, following criteria adapted from Unger et al. [9]: Samples located outside the LA or with a distance exceeding 100 mm were discarded. Samples' 1.5 s moving average filtered values were required to show "small oscillation" and "small absolute difference" in a window of 1 s. Thresholds of 180 Ω for IntellaNav Stablepoint™ and 210 Ω for IntellaNav Mifi™ accounted for sheath artefacts.

To assemble the blood pool, we selected samples iteratively based on the distal electrode's distance to the LA shell. For each map, an initial reference distance of 20 mm was chosen and iteratively reduced in 1 mm decrements until either a total of 70 samples adhering to the criteria were found or the reference distance fell below 7 mm. The patient specific minimal accepted distance (MAD) was computed by adding a 3 mm margin (as long as staying above 7 mm) to the maximum of terminal reference distances of all maps. Thereby, all preselected samples with distances greater than or equal to MAD were appended to a global array and weighted (w_i) based on their distance to their LA shell map (D2S). The patient-wide LI_{BP} was then calculated considering a total of L points:

$$LI_{\mathrm{BP}} = \frac{\sum_{i=1}^{L} w_i \cdot \mathrm{LI}_i}{\sum_{i=1}^{L} w_i}; \qquad \text{with } w_i = D2S_i - MAD + 1,$$

Point Processing

We derived a single LI value and location from the grouped samples and catheter electrode positions for each ablation point meeting the following reliability criteria. Ablation points with the distal electrode more than 6 mm from the LA shell for the recorded sample with "Ablation On" comment (ON-sample) were removed considering the mean relative motion of the catheter to the atrial wall, potential wall deformations, and map resolution limitations. If not stated differently, it is referred to values filtered with a 1.5 s moving average. Based on a priori knowledge of the range of LI and conductivity, only points with ON-sample values below 135% of the LI_{BP} were accepted to mitigate artifacts. When available, contact force served as an additional check, with values below 5 g indicating potentially poor catheter-tissue contact [8].

Sample selection ensured a stationary catheter position, requiring the distal electrode of the catheter to remain within an area of 6 mm Euclidean distance of the ON-sample location. To ensure stability, a threshold was set to the LI value of the ON-sample ± 2.5% of the LI_{BP}. Samples were considered up to the first threshold transgression by the moving average filtered data. If at least 20 samples remained, the mean location and the median LI value were calculated and extracted as the

location and value of the ablation point. To prevent superimposed spatial inaccuracy, the proximity of the calculated location to the LA shell was re-evaluated, excluding points with a distance over 6 mm. To ensure comparability with LGE-MRI values, we only examined substrate properties that were not altered by previous ablation. For every ablation the 10 nearest neighbors on the LA shell map were annotated as ablated, accounting for the catheter's diameter. However, if any point within this point cloud was previously annotated as ablated, the current point was excluded from the comparison.

Due to the absence of ground truth, three categories for point usability, differently accounting for interference between ablation points, were compared against each other. The first, considering all ablation points annotated as the first ablation (all 1^{st} Abl), the second, additionally requiring LI>LI_{BP}+8 Ω, and the third category, additionally excluding points if they fell within a safety area with a radius of 6 mm surrounding previously ablated points potentially indicating edema.

2.3 Point Registration and Comparison

For data comparison, one global mean shape was generated with Scalismo (Scalable Image Analysis and Shape Modelling Software) utilizing all patient geometries of both modalities. The process was adapted from Nagel et al. [5] and involved rigid alignment, establishment of point-wise inter-object association (correspondence), and creation of a continuous deformation field. The learned shape variations were stored in a low-rank Gaussian process isomorphic to a reference mesh which, when the Gaussian process' parameters were set to their mean value, coincided with the mean shape.

Next, IIR and normalized local impedance (LI_{N}) were co-registered through backward and forward registration to mean shape instances, respectively, entailing iterative closest-point alignment, establishment of correspondence using Gaussian processes, and transfer of corresponding value information. To determine a satisfactory average fit, a threshold of 3 (unitless, order of mm) was set for the Chamfer distance of both monomodal maps to the mean shape. To minimize information loss for the denser IIRs, the k nearest points were interpolated, with $k = \lfloor \frac{\#points_{\text{MRI}}}{\#points_{\text{MS}}} \rceil$. Comparison was done for each location with an LI value if the directional distance from the particular point to the fitted instance of the mean shape model for LI, and conversely, from the fitted mean shape to the nearest point in the IIR map, was below 4.5 (unitless, order of mm). The final IIR assignment included the 10 nearest neighbors and was conducted either by calculation of the median of all 10 nearest neighbours (med_{all}) or of the median of those points belonging to the majority category among the 10 individually characterized nearest neighbors (med_{maj}).

3 Results

Acknowledging the absence of a ground truth for substrate properties, we categorized points as "healthy", "interstitial fibrosis", or "dense scar" based on IIR thresholds.

Intra-Patient-Comparison

When examining individual patients, the analysis focused on the variability within LI_{N} values within one IIR category and the variability of LI_{N} data between IIR categories. Presenting results for all 1^{st} Abl contains the most possible data points for comparison. Limited data points (<10) in multiple patients necessitated evaluation based on representative cases. While some patients had only one category (healthy) represented, others featured points from all IIR categories. Inside one representative patient, LI_{N} values ranged from -0.04 to 0.34 for healthy and scar tissue, there was one single value for fibrosis.

Inter-Patient-Comparison

Including all patients' points, all methods of point usability assessment were considered. Considering edema, there were 6 healthy and one scar point; all points ranged from 0.06 to 0.3. For the other two usability categories resulting point quantities (#p) and bar plots of values are presented in Figure 2.

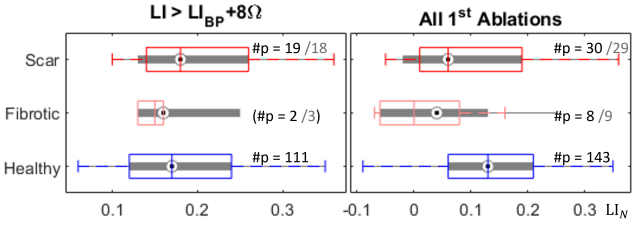

Fig. 2: Barplots for LI_{N}, showing median, 25 and 75%-iles and ranges. IIR assignment was done using med_{all} (colors) or med_{maj} (grey). Point quantities (#p) are given in corresponding order.

Points were primarily located adjacent to the pulmonary veins. Different IIR assignment methods led to partially different results. The limited data set precluded robust statistical analysis when considering edema or for fibrosis in the case of LI>LI_{BP}+8 Ω. IIR medians of healthy and fibrotic all 1^{st} Abl data differ significantly at the 5% significance level when using med_{all} but not with med_{maj}. For all 1^{st} Abl we employed Tukey's HSD test to assess mean differences. Healthy and fibrotic point groups show a p-value of 0.0058 for med_{all} and of 0.0124 for med_{maj}; all other intra-category mean differences are greater than 0.1. Notably, different IIR assignments, as well as consideration of means instead of medians led to a difference in the significance of results, particularly when comparing healthy versus fibrotic areas in all 1^{st} Abl.

4 Discussion

The primary finding of our study is the wide variation in results based on diverse criteria combinations and their significant impact on data processing and analysis outcomes, highlighting the need for cautious interpretation. We observed limited informative value in the results, emphasizing the necessity for statistical analysis beyond p-values and intra-group deviation. Notably, the same dataset was found to exhibit both significant and non-significant correlations depending on criteria selection. Due to overlapping unquantified influences, we could not draw any conclusions regarding the potential interdependence of LI and LGE-MRI data of LA tissue.

The substantial deviation of LI_N values within individual patients suggests that the LI_{BP} is not the only challenge for conclusive substrate characterization by LI. Yet, the LI_{BP} calculation reflects a tradeoff between sample quantity and reliability. Skepticism regarding the trustworthiness of LI_{BP} is raised by its composite nature, unclear influences of surrounding structures, and by LI values below LI_{BP}. Due to the overall reduced statistical robustness of the results, the comparison of all 1^{st} Abl with or without exceeding LI_{BP} by 8Ω did not yield conclusive evidence. Therefore, ad-hoc LI_{BP} measurements before the ablation delivery are advisable for comparing LI data.

The importance of conservative criteria for data reliability was balanced against the loss of information content due to the reduction of data points. In the clinical setup, LI is primarily used as a validation technique for lesion delivery, which demands less accuracy and tracking than absolute value analysis. We could not conclude on the impact of influences or determine a criteria combination yielding enough reliable data to assert a potential correlation. Thus, more trusted LI measurements are needed to infer a potential correlation. If ethically justifiable, recording LI prior to any ablation could mitigate the vast point exclusion and enhance information content.

Further examination of deviations could involve repeated measurements in a single area, accounting for spatial inaccuracy by assessing large areas with homogeneous IIR, or separate analysis for different LA regions. Consistency by using a single catheter, measuring with uniform contact force, maintaining an upright orientation of the catheter to tissue, and tracking respiratory and cardiac motion could minimize variability in LI. In the short term, due to the high deviations observed in intraoperative LI, full replacement of LGE-MRI data by LI measurements for substrate assessment seems unlikely. Nonetheless, clinical studies with standardized protocols that ensure data quality are desirable. Such studies facilitate robust and meaningful investigation, contributing to a deeper understanding of interrelations that may lead to complementary diagnostics or improved treatment of atrial arrhythmias.

5 Conclusion

Our findings underscore the necessity for standardized protocols in data acquisition and processing to minimize uncontrolled confounders when comparing two substrate characterization methods such as LGE-MRI and LI.

Author Statement

Research funding: This work was supported by the European Union's Horizon 2020 research and innovation programme under the Marie Skłodowska-Curie grant agreement No 860974 (PersonalizeAF). Authors state no conflict of interest. Informed consent has been obtained from all individuals included in this study. The study was carried out according to the Declaration of Helsinki guidelines and the deontological code of local institutions. The study protocol was approved by the ethics committee of the hospital.

References

[1] E. M. Benito, A. Carlosena-Remirez, E. Guasch, et al. Left atrial fibrosis quantification by late gadolinium-enhanced magnetic resonance: a new method to standardize the thresholds for reproducibility. *EP Europace*, 19(8):1272–1279, 2016.

[2] S.-S. Bun, D. G. Latcu, T. Delassi, et al. Ultra-high-definition mapping of atrial arrhythmias. *Circulation Journal*, 80(3): 579–586, 2016.

[3] G. Caixal, F. Alarcón, T. F. Althoff, et al. Accuracy of left atrial fibrosis detection with cardiac magnetic resonance: correlation of late gadolinium enhancement with endocardial voltage and conduction velocity. *EP Europace*, 23(3):380–388, 2020.

[4] I. García-Bolao, P. Ramos, A. Luik, et al. Local impedance drop predicts durable conduction block in patients with paroxysmal atrial fibrillation. *JACC: Clinical Electrophysiology*, 8(5): 595–604, 2022.

[5] C. Nagel, S. Schuler, O. Dössel, et al. A bi-atrial statistical shape model for large-scale in silico studies of human atria: Model development and application to ecg simulations. *Medical Image Analysis*, 74:102210, 2021.

[6] D. Nairn, M. Eichenlaub, B. Müller-Edenborn, et al. Differences in atrial substrate localization using late gadolinium enhancement-magnetic resonance imaging, electrogram voltage, and conduction velocity: a cohort study using a consistent anatomical reference frame in patients with persistent atrial fibrillation. *Europace*, 25(9), 2023.

[7] J. Pellman and F. Sheikh. Atrial fibrillation: Mechanisms, therapeutics, and future directions. 10.1002/cphy.c140047, 2015.

[8] F. Solimene and F. Maddaluno. Application of the intellanav stablepoint™ ablation catheter featuring contact force and local impedance information to treat ventricular ischemic substrate. DINEP2304EA, 2021.

[9] L. A. Unger, L. Schicketanz, T. Oesterlein, et al. Local electrical impedance mapping of the atria: Conclusions on substrate properties and confounding factors. *Frontiers in Physiology*, 12, 2022.